

Probing the sp^2 dependence of elastic moduli in ultrahard diamond films

M. G. Fyta¹, G. C. Hadjisavvas², and P. C. Kelires

Physics Department, University of Crete, P.O. Box 2208, 710 03, Heraklion, Crete, Greece

Abstract

The structural and elastic properties of diamond nanocomposites and ultrananocrystalline diamond films (UNCD) are investigated using both empirical potentials and tight binding schemes. We find that both materials are extremely hard, but their superb diamondlike properties are limited by their sp^2 component. In diamond composites, the sp^2 atoms are found in the matrix and far from the interface with the inclusion, and they are responsible for the softening of the material. In UNCD, the sp^2 atoms are located in the grain boundaries. They offer relaxation mechanisms which relieve the strain but, on the other hand, impose deformations that lead to softening. The higher the sp^2 component the less rigid these materials are.

Key words: carbon, ultrananocrystalline diamond, amorphous materials, nanocomposite, grain boundaries, elastic properties

1 Introduction

Carbon is an extraordinary chemical element. Its ability to form a variety of hybridized bonds leads to a plethora of structures with different properties. It is involved in most of the organic compounds in nature, but it is also the basic building block of many inorganic compounds and materials which are important for technological purposes. For example, diamondlike carbon structures have attracted intense research in both the fundamental and practical level.

¹ Present address: Department of Physics, Harvard University, 17 Oxford Str., Cambridge, 02138 MA, USA.

² Present address: Department of Physics & Astronomy, Vanderbilt University, 6631 Stevenson Center, Nashville, TN 37235, USA.

Pure carbon films that contain a high fraction of sp^3 diamondlike local geometries are potential candidates for incompressible and ultrahard materials. Examples of such materials, and the focus of the present study, are ultrananocrystalline diamond films and diamond nanocomposites. The realization of such materials is a promising route towards improving the mechanical properties of pure systems.

Ultrananocrystalline diamond (UNCD) films are about 1 μm thick and show high crystallinity (for a review see Ref. (1)). There seems to be only a small fraction of nondiamond phases (estimated below 5%). They possess a fairly uniform distribution of conglomerates made up of diamond crystallites with an average size between 3 and 5 nm. Crystallites larger than 10 nm are seen very occasionally, and these tend to be highly faulted and extensively twinned. Much work has been done, experimentally and theoretically, on the characterization of these films (2). The main issues are the details of the structure and the nature of the grain boundaries (GB) (3; 4). These could be twisted, tilted, amorphous or just disordered boundaries. Nevertheless, as long as the exact structure of the GB is not clear, their role in determining the properties of the film cannot be revealed. Regarding the atomistics, due to the fact that the crystallite size is limited to the nanoscale, the fraction of atoms located at the GB increases drastically with a decrease of the grain size. The presence of sp^2 atoms, together with the experimental fact that no graphitic phase was found between the GB suggests that the atoms are π -bonded across sharply delineated GB limited to widths of 0.2-0.5 nm.

Diamond nanocomposites ($n\text{D}/a\text{-C}$), on the other hand, consist of diamond crystallites that are embedded in an amorphous carbon ($a\text{-C}$) matrix. The appropriate choice of the size of the nanodiamond inclusion allows tailoring of the properties of the embedding medium. It has been recently shown that diamonds embedded in a tetrahedral $a\text{-C}$ ($ta\text{-C}$) matrix are both stable and highly incompressible materials, possessing elastic moduli higher than $ta\text{-C}$ (5). Their synthesis and growth mechanisms have been explored in both hydrogenated (6) and pure (7) $ta\text{-C}$ matrices.

In the present work, we further explore some of the elastic properties of both UNCD and $n\text{D}/a\text{-C}$, and try to correlate our findings to the microstructure of these materials. We mainly focus on the elastic parameters, such as the bulk and Young's moduli, which are evaluated at the equilibrium state and can provide information on the elastic response of the system to compression and extension, respectively. Due to computational limits the grains modeled were restricted to sizes up to 3 nm. These sizes may be smaller than the average size seen in the experiments, but as it will be shown in the next sections, the main features of the experimental findings are captured.

2 Methodology and Structural Characteristics

Here, we present results based on Monte Carlo (MC) simulations within the Tersoff empirical potential (EP) approach (8). This method provides a fairly good description of the structure and energetics of a wide range of *a*-C phases (9; 10), and superb statistical accuracy. We also present results based on Molecular Dynamics (MD) simulations, using the environment-dependent tight-binding (EDTB) model of Tang, Wang, Chan, and Ho (11), which provides superior accuracy in the energetics compared to the empirical schemes. This model allows the tight-binding parameters to change according to the bonding environment and has been successfully used in recent applications (12; 13). The use of both MC/EP and MD/EDTB schemes allows the treatment of large systems, and a check of the validity of the results by comparison to more accurate ones. Large supercells with up to about 10000 atoms are treated with the MC/EP method, while the smaller ones (less than 600 atoms) are modeled using the MD/EDTB scheme. Periodic boundary conditions are imposed on all supercells.

The *nD/a*-C structures contain a spherical nanocrystal in the middle, surrounded by dense amorphous carbon. They have been constructed, as previously reported (5), by applying the liquid-quench method to generate the amorphous matrix and by subsequently relaxing all the atoms at low temperatures. In the high density *nD/a*-C, where the nanodiamonds are embedded in a *ta*-C matrix (*sp*² fraction less than 30%), the majority of the local geometries are *sp*³ hybrids. It is essential in understanding the properties of such structures to take a closer look at the few *sp*² atoms and investigate the link between *sp*² fraction and nanodiamond size. We have previously found (5) that *sp*² sites are located in the *a*-C matrix, far from the interface between the matrix and the embedded nanodiamond, and form small clusters and chains, similar to the case of pure *ta*-C networks, where the clustering is also associated to stress relief (10).

The generation of the UNCD structures was done in a different manner. The concept of the Wigner-Seitz (WS) cell was used. The WS cell around a lattice point is defined as the set of points in space, which are closer to that lattice point than any of the other lattice points. The WS unit cell around a lattice point can be constructed by drawing lines connecting the point to all others in the lattice, bisecting each line with a plane, and taking the smallest polyhedron containing the point bounded by these planes (Fig.1a). In this way, starting from a cubic diamond configuration, imaginary lattice points are chosen in a bcc (fcc) structure and a large WS cell is constructed having the shape of a truncated octahedron (rhombic dodecahedron). The atoms inside the WS cell are removed, leaving an empty space in the interior of the cubic lattice. At a second step, another cubic diamond lattice is used, which is rotated

with respect to the first one (panel (b) in Fig.1). The same WS cell, as in the first step, is constructed and the atomic configuration contained in this cell is subtracted and embedded in the empty region of the first structure. In this way, misoriented polyhedra, simulating the diamond nanograins are generated. The grain sizes range from 0.7-3 nm. The final step is to fully relax the structure, both the atomic positions and the volume, at 500-1000 K, and then cool it to 0 K where properties are taken. The thin interface region between the fully relaxed misoriented grains are the grain boundaries (GB).

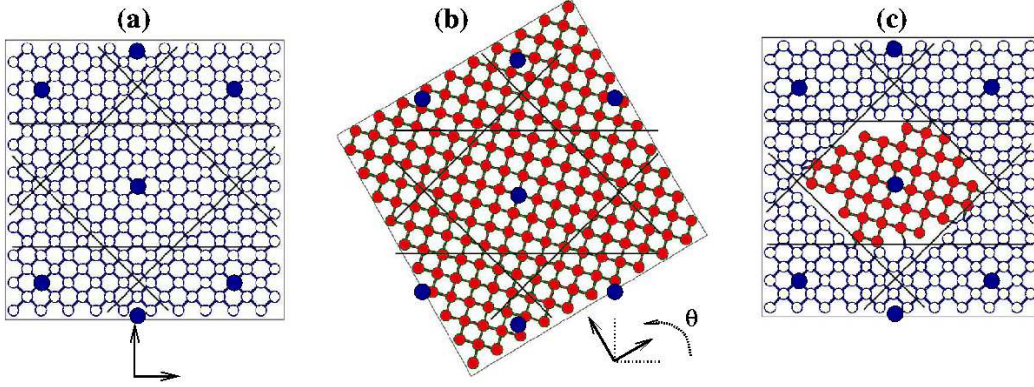


Fig. 1. Schematic representation of the construction of a nanodiamond cell. The large spheres denote the imaginary lattice points used to construct a WS cell by bisecting the lines which connect the central of these points to the others. (a) The atoms inside a WS cell are removed. The lattice in panel (b) has been rotated by an angle θ with respect to panel (a). The atoms of the second WS cell are embedded in the respective region of the first cell. The generated structure, before relaxation, is shown in (c).

Various random grain misorientations were tested during the generation of the UNCD cells. The angles were in the range of about 5-45 degrees. The criterion for accepting or rejecting the relaxed structures was the fraction of sp^2 sites. For a high percentage of threefold atoms (total number over 15-20 %) the films were considered as highly defective and deviated significantly from the experimental findings. The larger the rotation angles, the higher the number of the threefold atoms. This was actually expected, since for larger angles the mismatch between the neighboring diamond grains becomes larger, giving rise to more defects which are related to the threefold atoms. Another important issue is the grain size. For similar grain misorientations, the larger grains result in fewer threefold sites. Sizes below ~ 1 nm in general lead to unstable grains and very high disorder.

Taking a deeper look into the GB reveals some interesting features (Fig.2). These are randomly oriented, since the grain misorientations were randomly chosen. Rotation angles that would lead to well defined and studied twist or tilted boundaries were also chosen, but did not result in a relative low threefold fraction (3), suggesting that in UNCD the grains are possibly ran-

domly oriented. The sp^2 sites are located only at the grain boundaries. The material therein is rather disordered than amorphous and the GB cannot be described as tilted or twisted. In most cases, the average sp^2 component in the GB compared to the total number of atoms in the GB is $\sim 30\%$ (similar to experimental findings). The width of the GB is approximately 3-3.5 Å, again similar to experiment, and deformations are actually restricted in this area. This, of course, varies depending on the grain misorientations. For larger angles the width is larger, but the higher percentage of threefold bonding is related to more deformed boundaries. Inspection of Fig.2 reveals an additional feature. Small empty regions occur. The volume of these voids gets larger as the misorientations increase. The role of these voids is not completely clear, but they could possibly be related to stress relief regions and assist in the softening of the material. The above features are independent of the choice of the simulational method used.

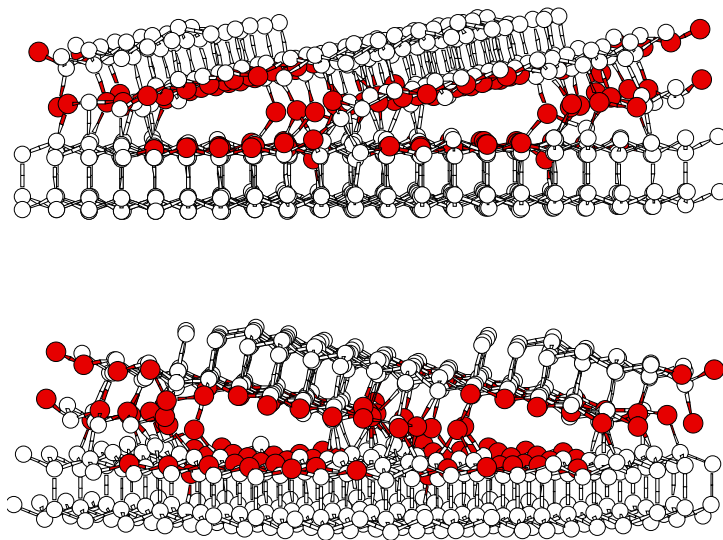


Fig. 2. Side views of randomly oriented grain boundaries in a nanodiamond cell. Open circles denote sp^3 hybridization, while the dark (red) ones are the sp^2 sites.

3 Elastic Moduli and sp^2 component

We now turn our attention to the elastic properties of the networks. As representative quantities, we compute the bulk modulus B and the Young's modulus Y . The former, is related to the response of the system to a volume change, due to variations in pressure. It is essentially a measure of a material's resistance to uniform compression. A common procedure for the calculation of the bulk modulus, which we also apply here uses the second derivative (with respect to the volume) of the Birch-Murnaghan isothermal equation of state (14) Within this theory the energy is given as an analytical function of the volume to which

we fit the energy versus volume curves extracted from our simulations. These are produced by varying the volume for each structure, allowing for relaxation in the atomic positions and calculating the corresponding energy. As a complement to B , the Young’s modulus serves as a measure of the stiffness of a material. It is defined as the rate of change of stress with strain (for small strains) and can easily be calculated through the second derivative of the energy with respect to the applied strain. For cubic systems, as the ones we deal with in this study, Y is also efficiently given through B : $Y = 3B(1 - 2\nu)$, with $\nu = \frac{c_{12}}{c_{11} + c_{12}}$; c_{11} , c_{12} are elastic constants calculated using volume conserving orthorombic, additionally to monoclinic strains (9). We refer to the cubic elastic moduli and accordingly derive Y , based on the fact that the supercells we use are large, the strains are small and the deviation from cubic symmetry negligible. The bulk modulus B for crystalline diamond calculated with ETDB and the Tersoff potential is 428 GPa and 443 GPa, respectively. We also consider the Wooten-Winer-Weaire (WWW) model (15), which is a fully tetrahedral structural model of a -C, i.e., a model of “amorphous diamond”, whose properties are an upper value for the corresponding properties of single phase a -C and serve as a comparison to the properties of the composites and UNCD. B of WWW is 360 (365) GPa using the Tersoff (EDTB) potential. Calculations of Y , or modulus of extension, with the Tersoff potential give values of 1060 GPa for diamond and 824 GPa for the WWW network (9).

We have recently shown using another tight-binding method that the elastic response of the nD/a -C networks to hydrostatic deformation is controlled by the nanoinclusions (5). Their bulk moduli are enhanced over the values for single phase a -C. The enhancement is stronger for dense composites (lower sp^2 component) and for larger diamond sizes. Here, we extend that analysis by confirming these results using different computational schemes and also including some calculations of the Young’s moduli. The results are shown in Table 1, divided in two parts. The left panel of the table represents the increase of the moduli for composites that contain a 1.7 nm nanodiamond, but differ in the sp^2 component of the matrix. The right panel shows results for composites with similar high density a -C matrices (sp^2 about 12%), that differ in the size of the nanodiamond they contain. Although the variation in the diamond sizes used was not very large it is clear from all simulations carried out and the range of grain sizes modeled, that both B and Y are strongly affected by the sp^2 content rather than the size.

The results obtained using the EDTB method are similar. A composite with a 1.05 nm diamond and matrix with a 30% sp^2 fraction has a bulk modulus of 300 GPa. The corresponding value for a pure a -C network with the same sp^2 fraction is about 12% lower. The same composite with a lower sp^2 component (11%) in the matrix has an even higher bulk modulus (357 GPa). Comparison with pure a -C reveals again that the modulus is about 11% higher. As the size of the diamond increases, the bulk modulus of the composite increases and it

is again enhanced compared to single-phase *a*-C. The modulus is 346 GPa for a 1.24 nm diamond embedded in an *a*-C matrix with 20% threefold atoms, which is increased about 16% over the *a*-C value.

Both schemes used, MC/EP and MD/EDTB, show very similar trends. The rigidity of the composites is considerably enhanced over that of pure *a*-C, and this is attributed to the presence of the diamond nanoinclusions. On the other hand, the increase of the sp^2 component in the matrix plays an important role in the lowering of the rigidity. As previously mentioned, the sp^2 atoms are mainly located far from the interface with the inclusion and form small chains and clusters. These clusters are known to be under tensile stress (9), providing relief of the overall compressive stress of the material, but they also provide softening mechanisms. Therefore, for an optimum performance of nanodiamond composite films, a balanced choice of size and density of nanoparticles and sp^2 content in the matrix is needed.

Table 1

Bulk and Young's moduli (in GPa) for various nD/a -C composites.

D=1.7 nm			sp^2 (%)=12		
sp^2 (%)	B	Y	D (nm)	B	Y
3.1	364	830	1.9	370	876
7.6	344	792	2.0	374	884
20.5	241	547	2.2	375	901

We next investigate the effect of the sp^2 component on the bulk and Young's moduli of various types of UNCD films. These threefold atoms, located in the GBs, are believed to control the elastic response of the films. The majority of the fourfold atoms in the grains are perfectly tetrahedral. A small fraction of sp^3 sites, located in the vicinity of the GBs are slightly distorted. Therefore, they are not expected to play a significant role in softening the material in comparison to crystalline diamond. Also, as previously mentioned, the voids that occur in the GB, due to grain misorientations, could also assist in softening. For small grain misorientations, these voids are not expected to greatly affect the properties, but should possibly play an important role for large misorientations, in which cases the softening is more evident.

The bulk and Young's moduli for UNCD structures with a fixed grain size (2.8 nm) and different grain orientations, leading to various sp^2 contents in the GBs, are plotted in Fig.3. All moduli are lower than diamond's but still very high, justifying the consideration of UNCD films as candidates for ultra-hard MEMS/NEMS components. The moduli are higher than those of pure *a*-C with similar threefold component, as well as those of the WWW "amorphous diamond" network. UNCD structures with low sp^2 component possess Young's moduli over 900 GPa. The reported experimental values are in the

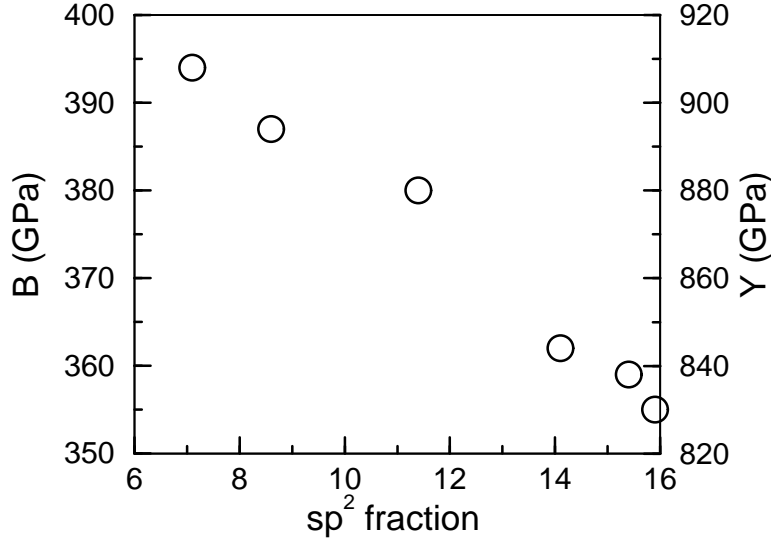


Fig. 3. Bulk and Young's moduli for UNCD films with grain sizes of 2.8 nm with varying sp^2 components (from MC/EP calculations).

range of 840-950 GPa, in very good agreement with the present theoretical predictions. It is clearly shown in this graph, that the sp^2 atoms formed due to the grain misorientations control the moduli. A structure that consists of 2.8 nm grains has a sp^2 fraction of 10% and a bulk modulus of 379 GPa, while values for 1.4 nm grains are 13% and 365 GPa, respectively. The grain misorientations were randomly chosen. The aim was not to simulate specific grain boundaries, but to investigate how the random misorientations determine the sp^2 fraction and thereby the properties of the material. In this way, not all the possible types of GB have been examined, and not the whole region of the experimentally produced grain sizes was spanned. Nevertheless, the good comparison to experimental data indicates that the main features related to the sp^2 content in UNCD films are well captured, and this work can serve as a first step to further explore these films.

The connection of the moduli to the sp^2 sites in the GBs is also confirmed through the EDTB calculations, although smaller grain sizes (~ 0.7 -1.4 nm) were simulated in this case. In addition, the dependence on the grain size was explored. For example, a UNCD film that consists of 1.4 nm grains with a misorientation around 15 degrees, has a threefold component $\sim 8\%$ and a bulk modulus of 310 GPa. This value is considerably lower than the value of over 380 GPa computed for a nanograin size of 2.8 nm in Fig. 3. The large difference is attributed to the small size of the grains which becomes comparable to the GB size. Thus, our simulations (both MC/EP and MD/EDTB) show that not only the grain misorientations have to be small, but also the grains should be larger than 2 nm. We believe that model UNCD structures with such characteristics (low sp^2 component, high phase purity and high elastic moduli) realistically simulate experimental UNCD films

Finally, we compare the elastic moduli of similar, in terms of their sp^2 component, nD/a -C and UNCD films. At low sp^2 components, the moduli of UNCD structures are undoubtedly higher than those of nD/a -C composites. However, the moduli of UNCD decrease more abruptly as sp^2 content increases (see variation in Fig. 3). Thus, it seems that for optimum UNCD films, the sp^2 content in the GBs need to be less than 10 %. Further calculations are required to unambiguously establish the link between sp^2 component and GB structure. This includes the consideration of a wider range of GB types and grain sizes. From a technological point of view, our results prove expedient in the quest for novel carbon materials and serve as a guide toward engineering diamond films with desired properties. Specifically, we provide a pathway to manipulate the mechanical properties of crystalline diamond by efficiently choosing the grain size and controlling the sp^2 content in the structure.

4 Conclusions

We have studied in this work the link of the microstructure, especially the sp^2 component, to the elastic moduli of diamond nanocomposites and ultrananocrystalline diamond films, by employing complementary MC/EP and MD/EDTB approaches. Both materials are found to be ultrahard, with moduli approaching those of diamond. UNCD films are superior when having low sp^2 component in the GBs. On the other hand, sp^2 sites are strain-relieving geometries in the GBs, so optimum values of sp^2 content are required. This depends on grain size and misorientation. For the same reason, a balanced choice of the sp^2 component is also needed in the case of diamond nanocomposites. Further work has to be devoted for the elucidation of this issue.

Acknowledgments

The authors wish to thank G. Kopidakis for providing access to his TBMD code. The work was supported by a grant from the EU and the Ministry of National Education and Religious Affairs of Greece through the action “ΕΠΕΑΕΚ” (programme “ΠΥΘΑΓΟΡΑΣ”).

References

- [1] D.M. Gruen, Ann. Rev. Mater. Sci. 29 (1999) 211.
- [2] L.C. Qin, D. Zhou, A.R. Krauss, and D.M. Gruen, Nanostr. Mater. 10 (1998) 649; P. Koblinski, S.R. Phillpot, D. Wolf, and H. Gleiter, Nanostr. Mater. 12 (1999) 339; S. R. Phillpot, D. Wolf, and H. Gleiter, J. App. Phys 78 (1995) 847.

- [3] P. Keblinski, D. Wolf, S.R. Phillpot, and H. Gleiter, J. Mater. Res. 13 (1998) 2077.
- [4] S.R. Phillpot, J. Wang, D. Wolf and H. Gleiter, Mater. Sc. Engin. A 204 (1995) 76.
- [5] M.G. Fyta, I.N. Remediakis, P.C. Kelires, and D.A. Papaconstantopoulos, Phys. Rev. Lett. 96 (2006) 185503.
- [6] Y. Lifshitz, T. Kohler, T. Frauenheim, I. Guzmán, A. Hoffman, R.Q. Zhang, X.T. Zhou, and S.T. Lee, Science 297 (2002) 1531; X.T. Zhou, Q. Li, F.Y. Meng, I. Bello, C.S. Lee, S.T. Lee, and Y. Lifshitz, Appl. Phys. Lett. 80 (2002) 3307.
- [7] Y. Yao, M.Y. Liao, T. Kohler, T. Frauenheim, R.Q. Zhang, Z.G. Wang, Y. Lifshitz, and S.T. Lee, Phys. Rev. B, 72 (2005) 035402.
- [8] J. Tersoff, Phys. Rev. Lett. 61 (1988) 2879.
- [9] P.C. Kelires, Phys. Rev. Lett. 73 (1994) 2460.
- [10] P.C. Kelires, Phys. Rev. B 62 (2000) 15686.
- [11] M.S. Tang, C.Z. Wang, C.T. Chan, and K.M. Ho, Phys. Rev. B 53 (1996) 979.
- [12] J.-Y. Raty, G. Galli, C. Bostedt, T.W. van Buuren, and L.J. Terminello, Phys. Rev. Lett. 90 (2003) 037401.
- [13] C. Mathioudakis, G. Kopidakis, P. C. Kelires, C. Z. Wang and K. M. Ho, Phys. Rev. B 70 (2004) 125202.
- [14] F.D. Murnaghan, Proc. Natl. Acad. Sci. U.S.A. 30 (1944) 244; F. Birch, Phys. Rev. 71 (1947) 809.
- [15] F. Wooten, K. Winer, and D. Weaire, Phys. Rev. Lett. 54 (1985) 1392; B.R. Djordjević, M.F. Thorpe, and F. Wooten, Phys. Rev. B 52 (1995) 5685.